0273-2289/92/3435—0613$02.40

Mass-Transfer and Kinetic Aspects in Continuous Bioreactors Using *Rhodospirillum rubrum*

J. P. COWGER, K. T. KLASSON, M. D. ACKERSON, E. C. CLAUSEN,* AND J. L. GADDY

University of Arkansas, Department of Chemical Engineering, Fayetteville, AR 72701

ABSTRACT

In designing bioreactors for the conversion of sparingly soluble gases, both mass transfer and kinetic effects must be considered. *Rhodospirillum rubrum,* an anaerobic photosynthetic bacterium capable of carrying out the water gas shift reaction, is an ideal organism for studying the relative importance of mass-transfer and kinetics since the cell concentration in continuous reactors employing *R. rubrum* may be regulated by the quantity of light supplied to the bacterium. This article addresses the performance of *R. rubrum* in continuous stirred-tank and trickle-bed reactors, with particular attention given to the importance of mass-transfer and reaction kinetics in modeling reactor performance. Estimates of mass-transfer coefficients are made for a trickle-bed reactor system based upon reactor performance equations and experimental observations.

Index Entries: *Rhodospirillum rubrum;* bioreactors; trickle-bed; carbon monoxide; photosynthetic.

NOMENCLATURE

C	liquid-phase concentration	(mol/mL)
f	fraction CO converted	(mol/mol)
G	volumetric gas flow rate	(mL/min)
H	Henry's law constant for CO	(mL atm/mol CO)

*Author to whom all correspondence and reprint requests should be addressed.

h	distance in column	(cm)
K_La	mass transfer coefficient	(min^{-1})
K_P	Monod constant	(atm)
L	volumetric liquid flow rate	(mL/min)
N	molar flow rate	(mol/min)
P	partial, total pressure	(atm)
q	specific CO uptake rate by cells	(mol/g,min)
R	ideal gas law constant	(mL atm/mol °K)
r_{CO}	volumetric uptake/transfer rate of CO	(mol CO/mL,min)
S	cross-sectional area of column	(cm^2)
T	absolute temperature	(°K)
V_L	liquid volume in CSTR	(mL)
X	cell concentration	(g/mL)
Y_{CO}	molar ratio of CO to inert	(mol CO/mol inert)
ϵ_L	liquid porosity in column	(mL/mL)
η	pressure drop/length in column	(atm/cm)

Superscripts

G	conditions in reaction
I	inlet conditions
O	outlet conditions
*	equilibrium value

Subscripts

Ar	argon
CO	carbon monoxide
L	liquid phase
m	maximum
t	total

INTRODUCTION

The biological production of H_2 is well documented, with a large number of organisms capable of utilizing a variety of organic substrates as electron donors for H_2 formation (*1*). *Rhodospirillum rubrum* and other nonsulfur purple bacteria have been shown to produce H_2 from organic substrates during growth in nitrogen-controlled cultures. It is believed that nitrogenase is responsible for the release of H_2 (*2,3*).

The production of H_2 by the water–gas shift reaction, as described in Eq. (1), by *Rhodopseudomonas gelatinosa* (now *Rhodocyclus gelatinosus*) was demonstrated by Tracy and Ashare (*4*):

$$CO + H_2O \rightarrow CO_2 + H_2 \quad (1)$$

This reaction is important in shifting synthesis gas from CO-rich to H_2-rich gas, since syngas is typically deficient in H_2 if chemicals production is desired. The capability of biological water–gas shift was initially only briefly mentioned for *R. rubrum* (*5*). However, the bacterium has more recently been utilized as a part of a tri-culture in converting CO to CH_4

through H_2 as an intermediate (*6*). *R. rubrum* is a photosynthetic bacterium that does not grow on CO, but utilizes a variety of other carbon sources for growth.

Since the substrate (CO) in Eq. (1) is a gas only sparingly soluble in the liquid medium, mass transfer becomes an important factor. A sufficient rate of transport must take place in order to supply the cells with CO. Typical reactors used in the gas–liquid systems include continuous-stirred tank reactors, gas lift reactors, and various types of column reactors.

Mass-transfer studies with *R. rubrum* are ideal for modeling bioreactors, since the cell concentration is dependent upon light supplied to the culture. Also, as mentioned previously, CO is not the limiting carbon substrate for growth. Instead, growth occurs on yeast extract, bicarbonate, or other carbon sources present in the liquid medium. Thus, various cell concentrations may be obtained by varying the liquid retention time and light supply in continuous culture.

The purpose of this article is first to demonstrate the use of *R. rubrum* in carrying out the water–gas shift reaction in continuous reactor systems. The specific characteristics of the bacterium are then utilized along with reactor performance equations in developing a new tool to probe reactor performance. The relative importance of mass-transfer and reaction kinetics is addressed.

MATERIALS AND METHODS

Rhodospirillum rubrum, ATCC 25903, was obtained from the American Type Culture Collection, Rockville, MD. The basal medium used in all experiments contained per liter of medium, 50 mL of Pfennig's minerals solution (*7*), 1 mL of Pfennig's trace metals solution (*7,8*), 5 mL of B-vitamins solution (*8*), 1 g of yeast extract (Difco), and 3.5 g of $NaHCO_3$. The medium was prepared in a 13.5-L Pyrex™ carboy (New Brunswick Scientific, New Brunswick, NJ), and steam sterilized at 2 atm (absolute) for 45 min. Cooling and removal of oxygen from the autoclaved medium were accomplished by bubbling a sterile mixture of N_2 and CO_2 (80/20%) through the medium prior to use. The cooled medium was reduced with 2 mL of $Na_2S{\cdot}9H_2O$ (2.5%)/L medium. Seed cultures for start-up were typically grown in large Erlenmeyer flasks using the same medium composition as described above.

Analytical Methods

Cell concentrations were estimated from optical density readings at 540 nm using a Spectronic 21 (Milton Roy Co., Rochester, NY) spectrophotometer and converting them to cell density using a calibration curve. A Perkin-Elmer (Norwalk, CT) Sigma 300 gas chromatograph and LCI-100 integrator were used for gas analysis. The 1.8m × 3 mm stainless-steel column was packed with Carbosphere (Alltech, Deerfield, IL), 60/80 mesh.

The temperature for the injector and thermal conductivity detector was 175°C, and the column temperature was 100°C. Helium was used as the carrier gas at a flow rate of 40 mL/min.

Equipment and Procedures

The cocurrent flow trickle-bed column reactor was constructed of plexiglass, and had an inside diamater of 5.1 cm and a packed height of 53.4 cm. Ceramic Intalox saddles with a 6 mm nominal diameter were used as packing. The culture and medium were continuously pumped through a recycle loop and into the reactor. After leaving the reactor, liquid and gas entered a gas–liquid disengaging vessel. After gas–liquid separation, the liquid was returned to the top of the reactor. An illumination chamber was inserted into the recycle loop to provide tungsten light to *R. rubrum*. Effluent culture was removed from the reactor using an overflow control, and fresh sterile medium was introduced to the reactor in the recycle loop. The liquid residence time was approx 24 h. Sterilization of the reactor was accomplished by using an ethylene oxide/carbon dioxide mixture (10/90% by wt) prior to inoculation.

The continuous-stirred tank reactor experiment was performed in a New Brunswick (New Brunswick, NJ) BioFlo II fermenter. The fermenter was equipped with temperature, pH, and agitation control. The fermenter had a working liquid vol of 1250 mL and an overhead gas vol of 350 mL. The agitation rate was held constant at 400 rpm, and illumination was supplied in a chamber similar to the one used in the trickle-bed studies. Cell broth was recirculated through the "light" chamber and returned to the reactor at a flow rate of 200 mL/min. Liquid feed and effluent were continuous, giving a liquid residence time of 24 h.

All experiments were carried out at 30°C and pH 7. The feed gas used was a mixture of H_2, Ar, CO, and CO_2 (20/15/55/10%) and was continuously fed to each reactor. Steady state was determined by observing no appreciable changes in CO conversion among several consecutive samples.

THEORY

The uptake of CO by *R. rubrum* involves mass transfer from the gas phase to the liquid phase and from the liquid phase to the cells. These effects work in combination with enzymatic reactions inside the cells. In a steady-state system, the volumetric rates for each effect must be equal:

$$r_{CO} = K_L a\,(C_L^* - C_L) = (K_L a / H)\,(P_{CO}^G - P_{CO}^*) = X\,q_m\,P_{CO}^* / (K_p + P_{CO}^*) \qquad (2)$$

In Eq. (2), $K_L a$ represents the overall mass transfer coefficient. The last term in the equation is the rate expression for CO uptake by the cells, which is independent of light supply and assumed to be represented by a Monod-type equation. A complete modeling study for the rate of CO up-

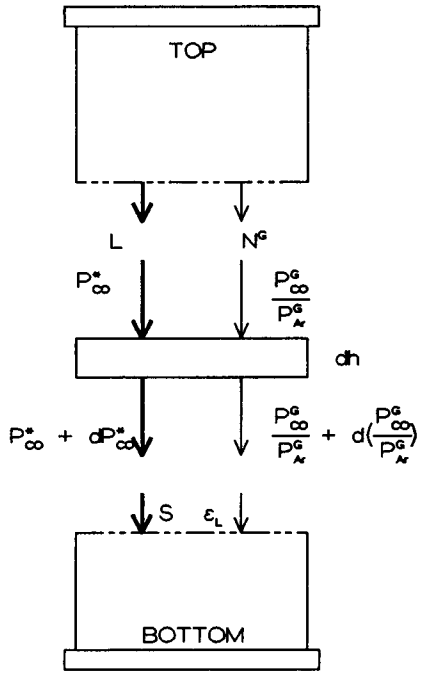

Fig. 1. Schematic of a slab in the trickle-bed reactor.

take by *R. rubrum* is to be published elsewhere (*9*). For a nonsteady-state system, the right-hand side of Eq. (2) will include a term for dissolved CO accumulation.

Trickle-Bed Reactor

For the specific case of a trickle-bed reactor, it can be shown that the partial pressure profiles for CO in the gas and liquid phases in the column are described by the following two differential equations:

$$(dY_{CO} / dh) = -(K_L a\, \epsilon_L / H)(P^G_{CO} - P^*_{CO})(S / N_{Ar}) \quad (3)$$

$$(dP^*_{CO} / dh) = (S / L)\{K_L a\, \epsilon_L (P^G_{CO} - P^*_{CO}) - [q_m P^*_{CO} / (K_p + P^*_{CO})] X H \epsilon_L\} \quad (4)$$

A representative schematic of a slab in a trickle-bed reactor may be found in Fig. 1. The derivation of Eqs. (3) and (4) was accomplished by setting up a mass balance for CO around this thin slab in the column. In addition to Eqs. (3) and (4), two more equations may be written describing the conversion of CO in the gas phase, and a relationship between molar gas flow rates and partial pressures. Fraction converted:

$$f = 1 - (Y_{CO} / Y^I_{CO}) = 1 - (P^G_{CO} / P^G_{Ar})(P^I_{Ar} / P^I_{CO}) \quad (5)$$

$$(N^G / N^I) = (P^I_{Ar} / P^G_{Ar})(P^G / P^I) = 1 + f(P^I_{CO} / P^I) \quad (6)$$

Equation (6) was derived by setting up a mass balance for CO in the gas phase from the column inlet to any position in the column. The stoichi-

ometry of the proposed reaction described in Eq. (1) was also incorporated into Eq. (6). As noted, the molar gas flow rate, N^G, at any point in the column increases with the conversion of CO. Equations (5) and (6) may be rewritten and solved for the partial pressures of CO and Ar (an inert gas added for material balance calcuations) in the gas phase:

$$P^G_{CO} = Y_{CO}\, P^l_{Ar}\, (P^G / P^l) / [1 + (P^l_{CO} / P^l) - Y_{CO}\, (P^l_{Ar} / P^l)] \quad (7)$$

$$P^G_{Ar} = P^l_{Ar}\, (P^G / P^l) / [1 + (P^l_{CO} / P^l) - Y_{CO}\, (P^l_{Ar} / P^l)] \quad (8)$$

Equations (3), (4), (7), and (8) may be used to describe the partial pressure profiles of CO and Ar along the column by solving the differential equations if the inlet conditions, reaction kinetics, pressure drop along the column, and mass-transfer properties are known.

If mass-transfer properties are sought, the above equations (Eqs. [1]–[8]) may be used with a few assumptions to yield an analytical solution. Assumption 1—an overall assumption that the molar flow contribution associated with dissolved CO is small compared to reaction rates and gas–liquid mass-transfer rates. This assumption is especially relevant for sparingly soluble species such as CO.

$$(L / H)\, (dP^*_{CO} / dh) \text{ is small} \quad (9)$$

Assumption 2—an overall assumption that the pressure drop in the column is linear.

$$P^G = P^l - \eta\, (h / h_t) \quad (10)$$

Assumption 3—cell concentration is constant throughout the column, which is justified at steady state and short liquid retention times (30–50 s).

Now, three analytical solutions are available based upon the following scenarios: (I) Mass transfer limiting conditions

$$P^G_{CO} >> P^*_{CO} \quad (11)$$

(II) Kinetic limiting conditions with

$$P^*_{CO} << K_p \quad (12)$$

(III) Kinetic limiting conditions with

$$P^*_{CO} >> K_p \quad (13)$$

Scenario I—$P^G_{CO} >> P^*_{CO}$: When $P^G_{CO} >> P^*_{CO}$, Eq. (3) may be written as:

$$N_{Ar}\, dY_{CO} = -(K_L a\, \epsilon_L / H)\, P^G_{CO}\, S\, dh \quad (14)$$

where $Y_{CO} = P^G_{CO}/P^G_{Ar}$. By noting that $N_{AR} = N^G\, (P^G_{Ar}/P^G)$ and substituting the expression for N^G from Eq. (6) into Eq. (4), Eq. (15) is obtained:

$$N^l\, [1 + f\, (P^l_{CO} / P^l)]\, (P^G_{Ar} / P^G)\, d\, (P^G_{CO} / P^G_{Ar}) = -(K_L a\, \epsilon_L / H)\, P^G_{CO}\, S\, dh \quad (15)$$

Equation (15) may be combined with Eq. (5), (10), and the ideal gas law to yield:

$$[1 + (P^I_{CO} / P^I) - (P^G_{CO} / P^G_{Ar})(P^I_{Ar} / P^I)](P^G_{Ar} / P^G_{CO})\, d\,(P^G_{CO} / P^G_{Ar})$$
$$= - (K_L a\, \epsilon_L / H)(SRT / G^I)[1 - (\eta h / P^I h_t)]\, dh \quad (16)$$

Finally, Eq. (16) may be integrated to yield:

$$[1 + (P^I_{CO} / P^I)]\, 1n\, [(P^I_{CO} / P^I_{Ar}) / (P^O_{CO} / P^O_{Ar})] - (P^I_{Ar} / P^I)$$
$$[(P^I_{CO} / P^I_{Ar}) - (P^O_{CO} / P^O_{Ar})] = (K_L a\, \epsilon_L / H)\, Sh_t RT\, [1 - (\eta / 2P^I)]\, (1 / G^I) \quad (17)$$

As noted in Eq. (17), a straight line should be obtained if the left-hand side is plotted as a function of $(1\text{–}0.5\ \eta/P^I)(1/G^I)$. The value of the slope should be proportional to $K_L a \epsilon_L$. The mass-transfer coefficient has here been written as $K_L a \epsilon_L$, which is standard for packed bed columns.

Scenario II—$P^*_{CO} << K_p$: If $P^*_{CO} << K_p$, Eq. (2) may be reduced to obtain Eq. (18):

$$r_{CO} = (K_L a / H)(P^G_{CO} - P^*_{CO}) = (X\, q_m\, P^*_{CO} / K_p) \quad (18)$$

which then may be combined with Eq. (3) to yield Eq. (19):

$$N_{Ar}\, dY_{CO} = - \{1 / [H / (K_L a\, \epsilon_L) + K_p / (q_m\, X\, \epsilon_L)]\}\, P^G_{CO}\, S\, dh \quad (19)$$

Equation (19) is of the same form as Eq. (14). Thus, the final equation may be written as (compare to Eq. [17]).

$$[1 + (P^I_{CO} / P^I)]\, 1n\, [(P^I_{CO} / P^I_{Ar}) / (P^O_{CO} / P^O_{Ar})] - (P^I_{Ar} / P^I)$$
$$[(P^I_{CO} / P^I_{Ar}) - (P^O_{CO} / P^O_{Ar})] = \{1 / [(H / (K_L a\, \epsilon_L)) + (K_p / (q_m\, X\, \epsilon_L))]$$
$$Sh_t RT\, [1 - (\eta / 2P^I)\, (1 / G^I) \quad (20)$$

Again, a straight line should be obtained if the same type of plot as mentioned in Scenario I is constructed. The value of the slope is now, however, dependent upon both $K_L a \epsilon_L$ and the cell concentration, X.

Scenario III—$P^*_{CO} >> K_p$: If $P^*_{CO} >> K_p$, Eq. (2) reduces to:

$$r_{CO} = (K_L a / H)(P^G_{CO} - P^*_{CO}) = q_m X \quad (21)$$

and Eq. (3) may be written as:

$$N_{Ar}\, dY_{CO} = - q_m\, X\, \epsilon_L\, S\, dh \quad (22)$$

A straightforward integration, along with application of the ideal gas law to N_{Ar}, yields:

$$(P^I_{CO} / P^I_{Ar}) - (P^O_{CO} / P^O_{Ar}) = [q_m\, X\, \epsilon_L\, S\, R\, T\, h_t / P^I_{Ar}]\, (1 / G^I) \quad (23)$$

In this case, a plot of the left-hand side of Eq. (23) as a function of $(1/G^I)$ should yield a straight line. The slope of the straight line is proportional to the cell concentration, X.

To summarize, even though analytical solutions may be obtained for the three different scenarios, it is impossible to determine if any one experiment is mass-transfer or kinetic limited. For instance, Scenarios I and II yield the same final equation for a mass-transfer and a nonmass-transfer

limited case. In light of this fact, it is necessary to conduct experiments with different cell concentrations. Then, if identical gas conversions are obtained, mass-transfer limiting conditions apply, and Eq. (17) may be used to find $K_L a \epsilon_L$. If, however, the conversion is affected by cell concentration, kinetic limitations are expected, and either Scenarios II or III may be studied further. Scenario II may allow determination of the overall resistance to CO uptake of a specific system, and Scenario III could yield information about q_m.

CSTR

The overall steady state CO balance over the CSTR may be written as:

$$(P^I_{Ar}\, G^I / RT)\,[(P^I_{CO} / P^G_{Ar}) - (P^G_{CO} / P^G_{Ar})] = r_{CO}\, V_L \tag{24}$$

where r_{CO} is the CO mass-transfer/uptake rate as defined in Eq. (2). If the first assumption is maintained, a similar discussion as with the trickle-bed reactor will yield the following final equations. Scenario I—$P^G_{CO} >> P^*_{CO}$:

$$(P^I_{CO} / P^G_{CO}) - (P^I_{Ar} / P^G_{Ar}) = (K_L a / H)\, V_L\, RT\, (1 / G^I) \tag{25}$$

Scenario II—$P^*_{CO} << K_p$:

$$(P^I_{CO} / P^G_{CO}) - (P^I_{Ar} / P^G_{Ar}) = \{V_L\, RT / [(H / K_L a) + (K_p / (q_m X)]\}\, (1 / G^I) \tag{26}$$

Scenario III—$P^*_{CO} >> K_p$:

$$(P^I_{CO} / P^G_{Ar}) - (P^I_{CO} / P^G_{Ar}) = (q_m\, X\, V_L\, RT / P^I_{Ar})\, (1 / G^I) \tag{27}$$

As is noted above, both Scenarios I and II result in similar equations indicating that a straight line should be obtained if $(P^I_{CO}/P^G_{CO}) - (P^I_{Ar}/P^G_{Ar})$ is plotted as a function of $1/G^I$. The slope of the line is either proportional to the mass transfer coefficient (Scenario I) or is a function of the cell concentration (Scenario II). Eq. (27), used with Scenario III, also indicates the effect of cell concentration on outlet conditions in the gas phase. Thus, no definite information about the mass-transfer coefficient value may be obtained from only one experiment. Multiple experiments must be conducted with various cell concentration levels to verify mass-transfer limiting conditions, which appear when further increases in cell concentration level do not affect gas conversion.

RESULTS AND DISCUSSION

Trickle-Bed Studies

The CO conversion is plotted as a function of the gas flow rate in Fig. 2 for four different experiments conducted in the trickle-bed reactor, where the liquid recycle rate and cell concentration were varied. The various cell concentration levels (100–370 mg/L) were obtained by changing the light

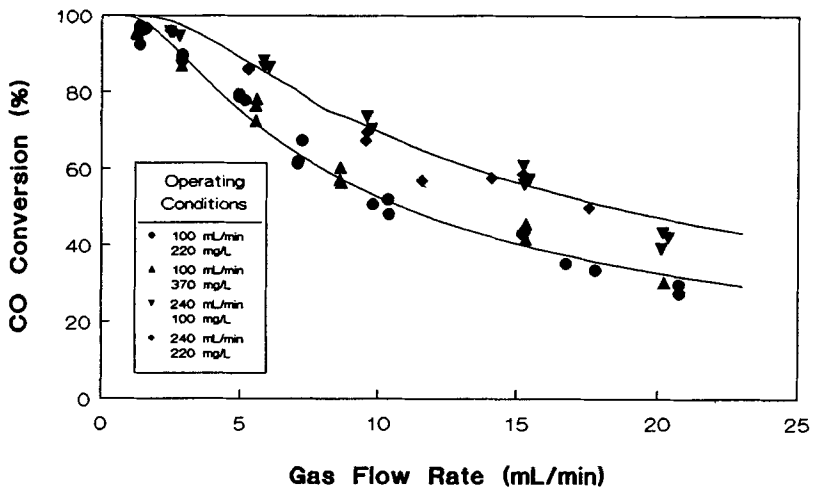

Fig. 2. Conversion of CO as a function of the gas flow rate in the trickle-bed reactor.

intensity in the "light chamber." A higher light intensity resulted in an increase in cell density in the system. Cell adherence to the surface of the packing was not observed to be appreciable, and thus, no corrections to cell density were necessary. As is noted in Fig. 2, the CO conversion was apparently not affected by the cell concentration, but changed with the liquid recycle rate. In the experiments conducted with a liquid recycle rate of 240 mL/min, a CO conversion of 70% was obtained for a gas flow rate of 10 mL/min, compared to a 50% CO conversion at the same gas flow rate and a liquid recycle rate of 100 mL/min. In accordance with the discussion in the previous section, it is clear that the main resistance in the uptake of CO lies in the mass transfer of CO to the cells, since CO conversion was not affected by cell concentration level. Thus, $K_L a \epsilon_L$ should be found by constructing the plot suggested in Scenario I.

In Fig. 3, the left-hand side of Eq. (17) is plotted as a function of the inverse of the gas flow rate. The slopes of the straight lines are proportional to the mass-transfer coefficient. Thus, the slope of 14.7 mL/min obtained for the experiments conducted with the higher liquid recycle rate indicates that the resistance to CO uptake is less in comparison to the runs using the lower recycle rate with a slope of 8.7 mL/min. This is, of course, also substantiated by the results presented in Fig. 2, where the higher liquid flow rate resulted in increased CO conversion (lower resistance).

By using the values of the constants listed in Table 1 and the values of the slopes in Fig. 3, $K_L a \epsilon_L$ may be calculated for the two different liquid recycle rates. Values of $K_L a \epsilon_L$ of 22 and 38 h^{-1} were found for liquid recycle rates of 100 and 240 mL/min, respectively. Based upon these estimates of $K_L a \epsilon_L$, the CO conversion was calculated using Eqs. (5) and (17) for the entire gas flow rate range studied. These obtained data were then used to construct the solid lines presented in Fig. 2. As is noted in the figure,

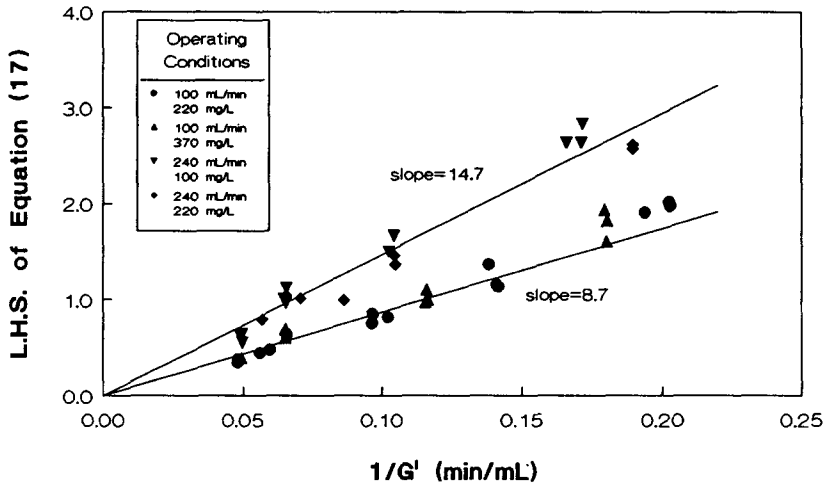

Fig. 3. Method of finding mass-transfer parameters for the trickle-bed reactor experiments.

Table 1
Constants Used in Calculations

H	= 1.120 mL·atm/mol CO (*10*)
R	= 8.206×10^{-5} mL·atm/mol·K
T	= 303°K
S	= 20.4 cm^2
h	= 51.5 cm
V_L	= 1250 mL
η	= 0, pressure drop negligible

good agreement was obtained between experimental data and predicted conversions. The values of $K_L a \epsilon_L$ found in the present system are of the same order of magnitude as reported in the literature. In using the correlation by Sherwood and Holloway (*11*) as modified by Goto and Smith (*12*) for predicting $K_L a \epsilon_L$ values in a trickle-bed reactor packed with glass beads (D = 4.13 mm), $K_L a \epsilon_L$ values of 10 and 14 h^{-1} may be calculated for the two liquid flow rates studies. These values correspond to the conditions in the present study, except for packing material. The diffusion coefficients needed in the correlation were estimated using well-known methods (*13*).

CSTR Studies

A single CSTR experiment was conducted in which the gas flow rate was varied with all other variables held constant. The CO conversion at a constant cell concentration of 400 mg/L is plotted as a function of gas flow rate in Fig. 4. In order to determine the possible limitations to CO uptake, the left-hand sides of Eq. (25)–(27) are plotted as a function of $1/G^I$ in Fig. 5. The theory predicts that the data should fall on a straight line for the applicable scenario. As is noted in Fig. 5, the experimental data fell on a straight line for Scenarios I and II. Plotting of the data according to Scenario

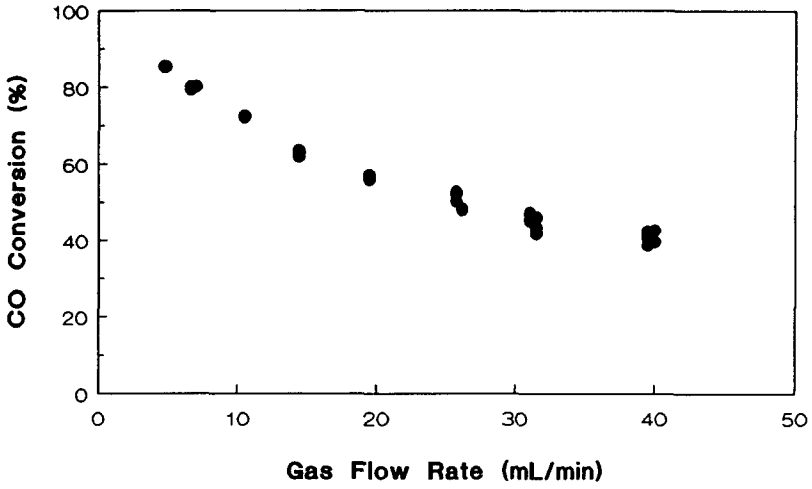

Fig. 4. Conversion of CO as a function of the gas flow rate in the CSTR.

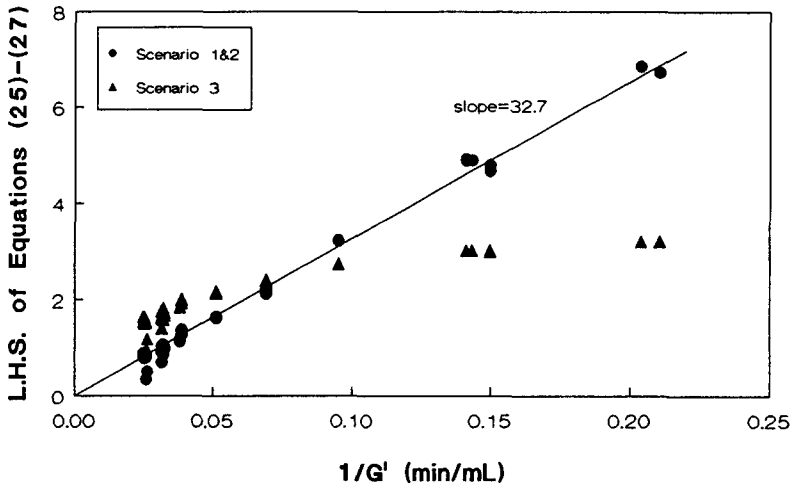

Fig. 5. Initial inspection to determine kinetic or mass transfer limitations in the CSTR.

III did not result in a linear relationship, indicating that kinetic limitations with $P^*_{CO} >> K_p$ are not likely in this experiment. The straight line fit of the data in Fig. 5 for Scenarios I and II suggests that the system is either under mass-transfer limitation or kinetic limitation with $P^*_{CO} << K_p$. The slope of the line was 32.7 mL/min. Future studies will include additional experiments at different cell concentration levels in order to yield further information about mass-transfer vs kinetic limitations.

CONCLUSIONS

Mass-transfer coefficients have been determined in a cocurrent trickle-bed reactor using a biological system with the photosynthetic bacterium

R. rubrum. Mathematical expressions were developed for the trickle-bed reactor and the continuous-stirred tank reactor in order to separate mass-transfer and kinetic limitations. These equations showed, as expected, that multiple experiments with various cell concentration levels must be conducted to yield definite conclusions regarding mass-transfer coefficients. The cell concentrations using *R. rubrum* were easily controlled by regulating the light supply. The experimental results showed that the mass-transfer coefficients were affected by liquid flow rates and that the values obtained were of the same order of magnitude as those found in the literature.

ACKNOWLEDGMENT

Financial support for the work was given by the US Department of Energy, Morgantown Energy Technology Center under contract DE-AC21-86MC23281.

REFERENCES

1. Gray, C. T. and Gest, H. (1965), *Science* **148(3667),** 186–192.
2. Nordlund,S. and Eriksson, V. (1979), *Biochim. Biophys. Acta* **547(3),** 429–437.
3. Vignais, P. M., Colbeau, A., Willison, J. C., and Jovanneau, Y. (1985), *Advances in Microbial Physiology,* vol. 26, Rose, A. H. and Tempest, D. W., eds., Academic, London, p. 155.
4. Tracy, C. A. and Ashare, E. (1983), *Biomethanation of Biomass Pyrolysis Gases,* Wise, D. L., ed., CRC Press, Boca Raton, FL, p. 107.
5. Dashekvicz, M. P. and Uffen, R. L. (1979), *Int. J. Sys. Bacteriol.* **29(2),** 145–148.
6. Klasson, K. T., Cowger, J. P., Ko, C. W., Vega, J. L., Clausen, E. C., and Gaddy, J. L. (1990), *Appl. Biochem. Biotechnol.* **24/25,** 317–328.
7. McInerney, M. J., Bryant, M. P., and Pfennig, N. (1979), *Arch. Microbiol.* **122(2),** 129–135.
8. Genthner, B. R. S., Davis, M. P., and Bryant, M. P. (1981), *Appl. Environ. Microbiol.* **42(1),** 12–19.
9. Klasson, K. T., Lundbäck, K. M. O., Clausen, E. C., and Gaddy, J. L. (1991), Kinetics of the Biological Conversion of Carbon Monoxide and Water to Carbon Dioxide and Hydrogen by *R. rubrum,* submitted for publication.
10. Faust, A. S., Wenzel, L. A., Clump, C. W., Mans, L., and Anderson, L. B. (1960), *Principles of Unit Operations,* John Wiley & Sons, New York, p. 552.
11. Sherwood, T. K. and Holloway, F. A. L. (1940), *Trans. Am. Inst. Chem. Eng.* **36,** 39–70.
12. Goto, S. and Smith, J. M. (1975), *AIChE Journal* **21(4),** 706–713.
13. Reid, R. C., Prausnitz, J. M., and Poling, B. E. (1987), *The Properties of Gases and Liquids,* 4th ed., McGraw-Hill, New York, p. 577.